

Understanding foraging behaviour in spatially heterogeneous environments

Glenn Marion^{a,*}, David L. Swain^b, Mike R. Hutchings^c

^a*Biomathematics & Statistics Scotland, James Clerk Maxwell Building, The King's Buildings, Mayfield Road, Edinburgh EH9 3JZ, UK*

^b*CSIRO Livestock Industries, JM Rendel Laboratories, Ibis Avenue, North Rockhampton, QLD 4701, Australia*

^c*Animal Biology Division, Scottish Agricultural College, West Mains Road, Edinburgh EH9 3JG, UK*

Received 17 July 2003; received in revised form 29 June 2004; accepted 4 August 2004

Available online 22 September 2004

Abstract

The role of stochasticity and spatial heterogeneity in foraging systems is investigated. We formulate a spatially explicit model which describes the behaviour of grazing animals in response to local information using simple stochastic rules. In particular the model reflects the biology in that decisions to move to a new location are based on visual assessment of the sward height in a surrounding neighbourhood, whilst the decision to graze the current location is based on the residual sward height and olfactory assessment of local faecal contamination. It is assumed that animals do not interact directly, but do so through modification of, and response to a common environment. Spatial heterogeneity is shown to have significant effects including reducing the equilibrium intake rate and increasing the optimal stocking density, and must therefore be taken into account by resource managers. We demonstrate the relationship between the stochastic spatial model and its non-spatial deterministic counterpart, and in the process derive a moment-closure approximation to the full process, which can be regarded as an intermediate, or pseudo-spatial model. The role of spatial heterogeneity is emphasized, and better understood by comparing the results obtained from each approach. The relative efficiency of random and directed searching behaviour in spatially heterogeneous environments is explored for both clean and contaminated pastures, and the impact of faecal avoidance behaviour assessed.

© 2004 Elsevier Ltd. All rights reserved.

Keywords: Animal behaviour; Resource distribution; Grazing systems; Spatio-temporal stochastic processes; Moment closure approximation

1. Introduction

Grazing systems represent approximately 20% of the total land area of the earth's surface (Hodgson and Illius, 1996). Environmental impact can be reduced by more efficient forage utilization, and grassland diversity enhanced through improved understanding of grazing selection. In addition the physical and economic productivity of a grazing system is intrinsically linked to the efficiency of a single grazing unit. Herbivore

utilization of grass swards is limited by the quality and quantity of forage ingested (Fryxell, 1991; Ungar, 1996), and the interaction between grazing animal and sward has important implications for the development of both. Therefore quantifying diet selection, herbage intake and modification of the forage resource base by the grazing animal will help define the limits to sustainable grazing systems.

There is widespread acknowledgment of key processes that determine grazing intake, these include bite rate, bite mass and grazing time (Laca et al., 1992; Ungar, 1996; Ungar and Noymeir, 1988). However, herbivores forage in spatially heterogeneous environments and make spatial choices to achieve their nutrient intake requirements, yet the impact of spatial heterogeneity on herbivore intake is poorly understood (Schwinning and

*Corresponding author. Tel.: +44-131-650-4898; fax: +44-131-650-4901.

E-mail addresses: glenn@bioss.ac.uk (G. Marion),
dave.swain@csiro.au (D.L. Swain),
M.Hutchings@ed.sac.ac.uk (M.R. Hutchings).

Parsons, 1999). Modelling stochastic foraging behaviour within spatially heterogeneous environments is emerging as an important tool for understanding grazing systems (Parsons et al., 2001). Deterministic modelling of herbivore grazing has provided valuable insights into the underlying processes that regulate plant–animal interactions. Methods, based on predator–prey interactions, which have used differential equations have the implicit and unrealistic assumption that grazing is a spatially homogeneous process (Noy-Meir, 1975). Recent developments have extended this approach to include bite scale patches with variable grazing intervals (Parsons et al., 2001; Schwinning and Parsons, 1999). However, these models fall short of being fully spatially explicit by assuming that animals defoliate bite-sized patches randomly irrespective of patch state or relative location. In practice the foraging animal's next bite or patch choice is determined by its location in relation to the spatial distribution of resources (see e.g. Grunbaum, 1998).

Herbivore behaviour can be captured by using a series of simple rules which they use when making grazing decisions in heterogeneous landscapes: (i) Select tall vegetative swards over short swards (Black and Kenney, 1984; Arnold, 1987; Bazely and Ensor, 1989; Bazely, 1990); (ii) Select nutrient rich swards over nutrient poor swards (Bazely, 1990; Langvatn and Hanley, 1993; WallisdeVries and Schippers, 1994) and (iii) select non-contaminated swards over faecally contaminated swards (Dohi et al., 1991; Hutchings et al., 1998). However, herbivores have incomplete knowledge of the local environment which creates a two stage grazing process within heterogeneous environments i.e. patch selection based on visual cues (e.g. sward height) and patch rejection based on more localized cues (e.g. olfactory cues associated with faeces). The relative strength of the cues will determine the grazing decisions (i.e. patch choice) of herbivores which will determine their nutrient intake rate, subsequent sward structure and thus the efficiency of use of the forage resource (Hutchings et al., 2002a).

Behavioural selection is in part determined by the physiological requirements of the grazing animal, the energy or nutrient demands of the animal will result in a strategic behavioural response. On this basis there has been a disproportionate amount of effort put into developing intake models that are demand driven (Yearsley et al., 2001). In practice these models have failed to deliver a generality which can be used beyond the specific conditions that they were constructed for. However, if intake is considered as a proxy for behavioural selection then the inverse of such a relationship should provide some insight into the limitations of grazing systems (Bao et al., 1998; Cazcarra and Petit, 1995; Gibb et al., 1998, 2002; Gordon et al., 1996; Illius et al., 1995). Although in practice there will be an interaction between demand and response, deriving a

basic set of response functions and exploring their limitations will help to explain some of the variability that exists within demand driven intake models.

This paper aims to improve the understanding of the interaction between foragers and their environment by formulating stochastic and spatially explicit models of animal behaviour. We demonstrate the importance of spatial heterogeneity in grazing systems and explore key elements of foraging behaviour in the spatial context. In addition, our treatment reveals the relationship between stochastic spatial models and their deterministic and non-spatial counterparts based on differential equations. In particular our approach builds on early predator–prey like models (Noy-Meir, 1975; Ungar and Noymeir, 1988) and the simple spatial models of Schwinning and Parsons (1999).

The model is developed through a series of stages to demonstrate the importance of behavioural selection within a spatial grazing environment. In the next section we introduce the mathematical concepts required in the remainder of the paper in the context of a simple foraging model. Section 3 develops our spatially explicit model of foraging behaviour, and Section 3.2 discusses resource management whilst issues related to animal behaviour are addressed in Section 3.3. The properties of the models are explored through simulation and by developing analytic approximations describing the evolution of the moments of the process; these are related to statistical properties of the system such as the spatial mean and variance of sward height. In particular, we discuss the relationship between stochastic spatial models and deterministic predator–prey like formulations. This process enables us to demonstrate how the approach we have adopted enhances understanding of grazing systems.

2. The importance of spatial heterogeneity

In order to address the issue of spatial heterogeneity in plant–animal interactions we begin with a simple deterministic non-spatial predator–prey like model. A spatial stochastic version of this model is constructed and we show how equations describing the moments of this process relate to the original non-spatial model. This approach provides useful insight into the role of spatial heterogeneity and simulations of the spatial system further develop this understanding. In addition to these concepts we introduce notation which is also used throughout the paper. We note that a number of earlier studies consider predator–prey like formulations (Noy-Meir, 1975; Ungar and Noymeir, 1988), and that the spatial stochastic process introduced in this section is broadly similar to models introduced by Schwinning and Parsons (1999). In subsequent sections we build on these foundations.

To begin consider the ordinary differential equation describing a simple foraging system

$$\frac{dg}{dt} = \gamma g - \beta cg, \quad (1)$$

where g is the average resource density, γ the growth rate of the resource, c the average density of foraging animals and β their feeding rate. The linear response βcg is supported by the observation that bite depth is proportional to sward height (Carrere et al., 2001). Nonetheless this is perhaps the simplest conceivable model of a foraging system, ignoring as it does spatial heterogeneity, stochasticity, interactions between individuals and non-linearity in resource growth or animal foraging behaviour. However, it serves as a useful starting point to analyse the impact of spatial heterogeneity in such systems. Solving for the fixed points of Eq. (1) we find that either $g = 0$, or for any resource density $g > 0$ the stable stocking density is

$$c^* = \gamma/\beta.$$

This system can be interpreted as a grazing model where g is the average sward height, γ the sward growth rate, c the average animal density, and β their bite rate. In this paper we focus on modelling grazing systems, however the insights gained shed some light on foraging systems in general.

To recast Eq. (1) as a spatial stochastic process, imagine that the area under grazing is divided into N patches. The sward height is g_i in patch $i = 1, \dots, N$ and the corresponding number of animals c_i . Both g_i and c_i are assumed to be integers. An animal may only graze its current location or move to a new location anywhere within the system (we consider local movement later). At patch i the probability of a bite being taken during a small time interval $(t, t + \delta t)$ is

$$P(g_i(t + \delta t) = g_i(t) - 1) = \beta c_i(t) g_i(t) \delta t,$$

where the sward height is measured in units of bite size and there is no variation in bite size. The probability of grass growth in patch i is given by

$$P(g_i(t + \delta t) = g_i(t) + 1) = \gamma g_i(t) \delta t.$$

So far this is simply a stochastic version of the deterministic non-spatial model (1) for N isolated patches. To link patches, introduce directed-searching by assuming that animals move preferentially towards taller swards (Black and Kenney, 1984; Arnold, 1987; Bazely and Ensor, 1989; Bazely, 1990), with the probability of movement from patch i to j in the time interval $(t, t + \delta t)$ being

$$P \begin{pmatrix} c_i(t + \delta t) = c_i(t) - 1 \\ c_j(t + \delta t) = c_j(t) + 1 \end{pmatrix} = \frac{v}{N} c_i(t) g_j(t) \delta t,$$

where v is the intrinsic directed-search rate. This model, with global searching directed toward taller swards, is similar to those considered by Schwinning and Parsons

(1999), but latterly we shall make the model truly spatially explicit by introducing local searching. If the g_j are thought of as resource quality then this search strategy can be interpreted as the selection of nutrient rich swards (Bazely, 1990; Langvatn and Hanley, 1993; WallisdeVries and Schippers, 1994). Note that all the event probabilities introduced above share the common structure

$$P(n(t + \delta t) = n(t) + \delta n) = R(n \rightarrow n + \delta n) \delta t, \quad (2)$$

where $R(n \rightarrow n + \delta n)$ represents the rate of an event causing the change δn in state space $n^T = (\{g_i, c_i : i = 1, \dots, N\})$. Given Eq. (2) the model can then be defined in terms of the event rates

$$\begin{array}{llll} R(n \rightarrow n + \delta n) & \delta g_i & \delta c_i & \delta c_j \\ \gamma g_i & +1 & 0 & 0 & \text{Growth at } i, \\ \beta c_i g_i & -1 & 0 & 0 & \text{Bite at } i, \\ v c_i g_j & 0 & -1 & +1 & \text{Move } i \rightarrow j. \end{array} \quad (3)$$

Taken together Eq. (2) and the event rates (3) describe a discrete state-space Markov process (Cox and Miller, 1965). Stochastic processes of this type have been widely used in modelling biological populations (Keeling et al., 2000; Bolker and Pacala, 1997; Renshaw, 1991), epidemics (Filipe and Gibson, 1998; Rohani et al., 2002), and chemical reactions (Van Kampen, 1992; Marion et al., 2002). Exact simulation is straightforward as the inter-event times are exponentially distributed (see e.g. Renshaw, 1991). Whilst an approximate alternative method results from updating time by a sufficiently small increment δt and allowing events to occur with probabilities given by Eqs. (2) and (3).

The relationship with the non-spatial deterministic system (1) can be seen if we consider the evolution of expectations in the stochastic model. First introduce the expectation of the spatial average

$$\langle z \rangle = E \left[\frac{1}{N} \sum_{i=1}^N z_i \right], \quad (4)$$

for any quantity z_i defined at each site $i = 1, \dots, N$. If $z_i(t)$ is a stochastic process then $\langle z(t) \rangle$ is the expected density over all sites, and over all realizations of the process, at time t . In the sequel we shall implicitly assume such time dependence, thus $\langle g \rangle$ is the expected average sward height over all the patches, and similarly $\langle c \rangle$ the expected average animal density, both at time t . The appendix shows how to derive equations describing the time evolution of these quantities. Given that the model contains neither animal mortality nor fecundity it is reassuring to note that $d\langle c \rangle/dt = 0$. Similarly evolution of the average sward height is governed by,

$$\frac{d}{dt} \langle g \rangle = \gamma \langle g \rangle - \beta \langle c \rangle \langle g \rangle - \beta \text{Cov}(c, g), \quad (5)$$

where the spatial covariance

$$\text{Cov}(c, g) = \langle cg \rangle - \langle c \rangle \langle g \rangle,$$

is a measure of the association between animals and the resource. If we identify $\langle g \rangle$ with the deterministic sward height g , and a constant $\langle c \rangle$ with the stocking density c , then for $\text{Cov}(c, g) = 0$ Eq. (5) corresponds to the deterministic model (1). In the spatial stochastic model positive correlation $\text{Cov}(c, g) > 0$ will increase the grazing pressure with respect to (1), whilst negative correlation will have the reverse effect. Fig. 1 shows the results from a simulation of the linear global directed-search model (2) and (3), alongside the corresponding output from the deterministic non-spatial model. The animal density is chosen to be the stable stocking density $c = \langle c \rangle = c^*$ of the non-spatial model. In the spatial system the correlation between the animals and the resource is initially zero, but quickly becomes negative as the animals deplete the local sward, the total intake rate is then below that expected from the deterministic model and the average height of the sward increases. However as the heterogeneity grows the animals select the taller swards, the correlation increases until $\text{Cov}(c, g) > 0$, and intake rate rises to an unsustainable level. Thus in the stochastic spatial model the system is over-grazed and the sward becomes extinct, which is in marked contrast to the results obtained from the non-spatial system (1). It is worth noting that for the case $N = 1$, the animals cannot move so $\text{Cov}(c, g) = 0$,

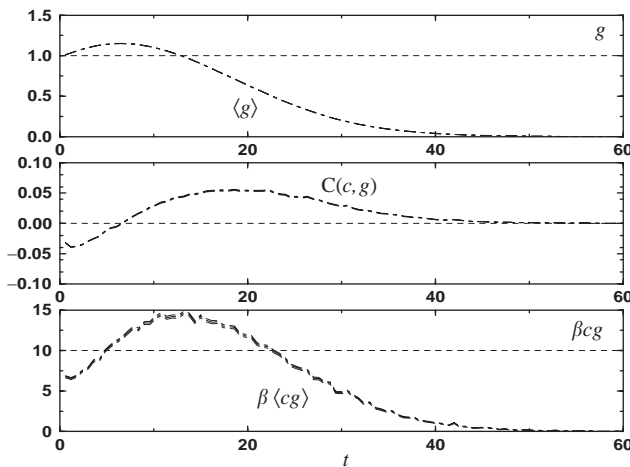


Fig. 1. Global directed searching. Results from the deterministic model (1) (dashed lines) for $g(0) = 1$, $\beta = 1$ and $\gamma = 0.1$, and a stable stocking density $c = 0.1$. The top graph shows the average sward height, the middle the normalized correlation $C(c, g)$ and the bottom the average intake rate. Means and ± 2 standard deviation confidence intervals (dot-dashed curves) from the stochastic spatial model (2) and (3) obtained by averaging 200 realizations of the process for 100 time points in the interval $t \in (0, 60)$. The simulations were performed on a 10×10 lattice with parameter values $\beta = 1$, $\gamma = 0.1$, and $v = 1$, with initially uniform sward with $\langle g \rangle = 1$ and with randomly distributed animals at stocking density $\langle c \rangle = 0.1$.

and simulation results show that this, essentially non-spatial, stochastic system is stable. Therefore, the behavioural response is a critical component when predicting intake rate, but it cannot be isolated from the spatial heterogeneity of the sward (Wilmschurst et al., 1999). These results demonstrate that spatial heterogeneity, which in this case is generated by individual behaviour, has the potential to radically alter the predictions of models of foraging systems.

3. A stochastic spatial model of grazing

The stochastic and spatial model of the previous section is broadly similar to the model introduced by Schwinning and Parsons (1999). The results clearly demonstrate the importance of individual behaviour and spatial heterogeneity in grazing systems. Moreover, our analytic treatment makes clear the relationship to non-spatial deterministic predator-prey like formulations. However, the model (2) and (3) is unrealistic in a number of respects. Firstly, the animals search for tall swards across the entire system. This becomes increasingly unrealistic as the size of the lattice grows and a more plausible alternative is that the animals search a local neighbourhood only. Accordingly, the search term is modified to

$$P \begin{pmatrix} c_i(t + \delta t) = c_i(t) - 1 \\ c_j(t + \delta t) = c_j(t) + 1 \end{pmatrix} = \frac{v}{z} c_i(t) g_j(t) \delta t \quad \forall j \in \mathcal{N}_i,$$

where the neighbourhood of i , \mathcal{N}_i contains z patches. In the following we assume a square lattice and a von-Neumann neighbourhood \mathcal{N}_i shown in Fig. 2 where $z = 4$ (except for those patches at the boundary). This reflecting boundary condition was chosen as it prevents the animals from being ‘stuck’ at the edges of the finite domain, and is more realistic than a toroidal boundary condition. Introducing this change results in a model where the average sward height diverges. This happens because the animals are less mobile than before and the linear rate allows ungrazed patches to grow

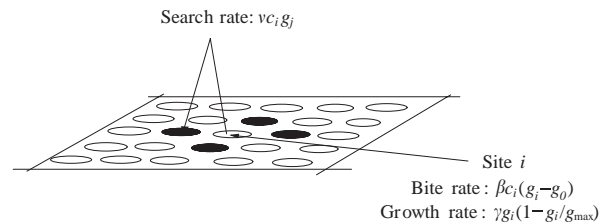


Fig. 2. Schematic representation of local directed-search model (2) and (6). This is a stochastic and spatial extension of the deterministic model (1) in which patches are linked via directed searching by foraging animals. The animals are assumed to search in some local neighbourhood $j \in \mathcal{N}_i$ shown here by the dark patches.

exponentially fast. The growth function is therefore modified to the more realistic self-limiting logistic form

$$P(g_i(t + \delta t) = g_i(t) + 1) = \gamma g_i(t)(1 - g_i/g_{\max})\delta t.$$

The choice of logistic growth also reflects the idea that growth rate varies with sward height and that there is an optimum height for cutting and regrowth as is well known to pasture managers (Johnson and Thornley, 1984). Despite this modification, simulations suggest that the system is still unstable with the sward now becoming extinct for a wide range of parameter values. This situation is rectified once we note that grazing animals typically graze the sward down to a certain minimum level, leaving an ungrazable portion to recover. For example, cattle typically graze swards down to 2 cm (Phillips, 1993). Thus the probability of a bite in patch i becomes

$$P(g_i(t + \delta t) = g_i(t) - 1) = \beta c_i(t)(g_i(t) - g_0)\delta t,$$

where g_0 is the ungrazable portion of the sward. This functional form gives rise to a linear relationship if we plot the average number of bites per visit to a patch against the sward height at the time an animal arrives in the patch. This is in accord with the behavioural observation that bite depth is proportional to sward height (Carrere et al., 2001). Clearly such a relationship holds only in a limited range to which we restrict ourselves here. However, it is anticipated that departures from linearity will be negligible where the sward height is sufficiently low, for example in heavily or moderately grazed systems. The above relationship also ignores the effect of intake requirements on the system, and in this paper we assume animals graze continuously. A further criticism of the model is that for the sake of simplicity the movement rate does not depend on the quantity of forage available at the current patch but only on that in neighbouring patches. However, it should be noted that although the movement rate is unaffected as the local forage availability increases the bite rate goes up and so the probability the next event is a move diminishes.

The model is summarized by the event rates which now read

$R(n \rightarrow n + \delta n)$	δg_i	δc_i	δc_j	
$\gamma g_i(1 - g_i/g_{\max})$	+1	0	0	Growth at i ,
$\beta c_i(g_i - g_0)$	-1	0	0	Bite at i ,
$\frac{v}{z} c_i g_j$	0	-1	+1	Move $i \rightarrow j \in \mathcal{N}_i$.

(6)

Eqs. (2) and (6) define the *local directed search model*.

As noted above the neighbourhood structure is defined on a square lattice with reflecting boundaries. Simulations based on an alternative formulation of this model in which the search distance is governed by a

power-law suggest that the results presented here are relatively insensitive to the precise geometry used. (i.e. similar results obtained if allow searching out to the next nearest neighbours). Additional simulations (not shown here) suggest that our results are relatively insensitive to the patch scale (i.e. the number of patches N). For example, with four animals $\gamma = \langle c \rangle, \beta = 1, v = 0.1, g_{\max} = 10$, and $g_0 = 1$ we found that the expected intake rate at equilibrium varied by less than 2.5% for $N \in (100, 900)$, and at least some of this variation is accounted for by the effective reduction in nearest-neighbour search distance as N increases. Therefore in the following we restrict our attention to the case $N = 100$.

3.1. Non-spatial and pseudo-spatial deterministic models

The non-spatial deterministic representation of this system is easily constructed by neglecting the site index i and the search rate in Eq. (6). Thus,

$$\frac{dg}{dt} = \gamma g \left(1 - \frac{g}{g_{\max}} \right) - \beta c(g - g_0), \tag{7}$$

is the generalization of Eq. (1) resulting from introduction of a minimum grazable portion g_0 , and logistic growth of the resource. In this section we develop a pseudo-spatial deterministic approximation to the stochastic spatial model (2) and (6) which reveals the relationship between the fully spatial stochastic system and Eq. (7).

As before equations describing the expectation of spatial averages can be derived from the full stochastic spatial model (2) and (6). As shown in the appendix the average animal density $\langle c \rangle$ is still constant,

$$\frac{d}{dt} \langle c \rangle = 0, \tag{8}$$

whilst now,

$$\begin{aligned} \frac{d}{dt} \langle g \rangle &= \gamma \left(\langle g \rangle - \frac{\langle g \rangle^2}{g_{\max}} \right) - \beta \langle c \rangle (\langle g \rangle - g_0) \\ &\quad - \frac{\gamma}{g_{\max}} \text{Var}(g) - \beta \text{Cov}(c, g), \end{aligned} \tag{9}$$

where $\text{Var}(g) = \langle g^2 \rangle - \langle g \rangle^2$. The deterministic and non-spatial counterpart to this model (7) corresponds to the case where the sward height is uniform, $\text{Var}(g) = 0$, and there is no association between animal location and the resource, $\text{Cov}(c, g) = 0$. In contrast, the discrepancy between (7) and (9) grows with the degree of spatial heterogeneity measured by $\text{Var}(g) > 0$ and $\text{Cov}(c, g) \neq 0$.

To determine spatial effects the variability across the system of both the resource $\text{Var}(g)$ and the animals $\text{Var}(c)$, and their covariance $\text{Cov}(c, g)$ must be

quantified. The appendix outlines the derivation of the following equations

$$\begin{aligned} \frac{d}{dt} \text{Cov}(c, g) &= (\gamma + \beta \langle c \rangle) \text{Cov}(c, g) + \frac{\gamma \langle c \rangle}{g_{\max}} \text{Var}(g) \\ &+ \beta g_0 \text{Var}(c) - \frac{\gamma}{g_{\max}} (\langle cg^2 \rangle - \langle c \rangle \langle g \rangle^2) \\ &- \beta (\langle c^2 g \rangle - \langle c \rangle^2 \langle g \rangle) + vz (\langle g(0)g(0)c(1) \rangle \\ &- \langle c(0)g(0)g(1) \rangle), \end{aligned} \quad (10)$$

$$\begin{aligned} \frac{d}{dt} \text{Var}(g) &= \gamma \langle g \rangle \left(1 - \frac{\langle g \rangle}{g_{\max}} \right) + \beta \langle c \rangle (\langle g \rangle - g_0) \\ &+ 2\gamma \left(1 + \frac{1}{g_{\max}} (\langle g \rangle - 1/2) \right) \text{Var}(g) \\ &+ 2\beta \left(g_0 + \langle g \rangle + \frac{1}{2} \right) \text{Cov}(c, g) \\ &- \frac{2\gamma}{g_{\max}} (\langle g^3 \rangle - \langle g \rangle^3) \\ &- 2\beta (\langle cg^2 \rangle - \langle g \rangle^2 \langle c \rangle), \end{aligned} \quad (11)$$

and

$$\begin{aligned} \frac{d}{dt} \text{Var}(c) &= 2vz (\langle g(0)c(1) \rangle + \langle c(0)g(0)c(1) \rangle \\ &- \langle c(0)c(0)g(1) \rangle), \end{aligned} \quad (12)$$

which describe the time evolution of these quantities. These expressions describe the expected values of spatial averages with fluctuations between different stochastic realizations being ignored. Note that the factors of z appearing above simply reflect the definition of the two-site terms (e.g. $\langle g(0)c(1) \rangle$) given in the appendix. Since we have ignored any boundary effects in this derivation it is anticipated that this approximation improves with the number of patches N , and the results presented below suggest that it is a good approximation for the moderately sized systems considered here.

Eqs. (9)–(12) describe the evolution of expectations of the first- and second-order statistics of the spatial system. Just as the evolution of $\langle g \rangle$ depends on the second-order terms $\text{Cov}(c, g)$ and $\text{Var}(g)$, and indirectly on $\text{Var}(c)$, so these depend on the *single-site* third-order quantities $\langle g^3 \rangle$, $\langle c^2 g \rangle$ and $\langle cg^2 \rangle$, and on *two-site terms* like $\langle g(0)c(1) \rangle$ (see appendix for definition), which account for correlations between nearest-neighbours. The evolution of these nearest-neighbour quantities are described in terms of interactions between next nearest-neighbours, which in turn depend on those between a site and the neighbours of its next nearest neighbours, and so on. We choose to close this infinite hierarchy simply by ignoring correlations *between* sites and thus writing two-site quantities as functions of single-site

terms as follows:

$$\begin{aligned} \langle g(0)c(1) \rangle &= \langle g \rangle \langle c \rangle, \\ \langle c(0)g(0)c(1) \rangle &= \langle cg \rangle \langle c \rangle, \\ \langle c(0)c(0)g(1) \rangle &= \langle c^2 \rangle \langle g \rangle, \\ \langle g(0)g(0)c(1) \rangle &= \langle g^2 \rangle \langle c \rangle, \\ \langle c(0)g(0)g(1) \rangle &= \langle cg \rangle \langle g \rangle. \end{aligned} \quad (13)$$

Similarly the third-order single-site terms $\langle g^3 \rangle$, $\langle c^2 g \rangle$ and $\langle cg^2 \rangle$ depend on fourth-order terms, and so on. Therefore following Keeling (2000a) assume that the state variables g_i and c_i are distributed log-normally across sites. As shown in the appendix this allows the following approximations to be made:

$$\begin{aligned} \langle c^2 g \rangle &= \frac{\langle c^2 \rangle \langle cg \rangle^2}{\langle c \rangle^2 \langle g \rangle}, \quad \langle cg^2 \rangle = \frac{\langle g^2 \rangle \langle cg \rangle^2}{\langle g \rangle^2 \langle c \rangle} \quad \text{and} \\ \langle g^3 \rangle &= \left(\frac{\langle g^2 \rangle}{\langle g \rangle} \right)^3. \end{aligned} \quad (14)$$

At present, for systems of more than one dimension, there are only a few distributional assumptions which allow closure to be obtained in a parametric form which for the log-normal takes the simple form shown above. In addition the log-normal has positive support and is therefore more appropriate than commonly used closure approximations such as the normal distribution (see e.g. Whittle, 1957; Marion et al., 2000; Keeling, 2000b). In Section 3.1.1 below we explore the validity of the log-normal distribution in the current context.

Applying the approximations (13) and (14) to the moment evolution equations (9)–(12) results in a log-normal approximation to the local directed search model. This can be regarded as an approximation to the full spatial stochastic process or used as a deterministic pseudo-spatial model in its own right. A similar attitude to an analytic approximation was adopted by Ferguson et al. (2001) in the context of modelling Foot and Mouth disease. In the remainder of this paper we refer to this approximation as the pseudo-spatial model or the log-normal approximation.

3.1.1. Validity of pseudo-spatial model

Figs. 3 and 4 compare this log-normal approximation with results obtained from the spatial stochastic process (9)–(14). Approximation of the average sward height $\langle g \rangle$ and the intake rate $\beta \langle cg \rangle$ are good, but that of $\text{Var}(g)$ and $\text{C}(c, g)$ are somewhat less convincing especially in Fig. 4 where the movement rate v is small relative to the bite rate β . Fig. 13 (to be discussed in detail later) clearly shows that the accuracy of the pseudo-spatial model increases with the directed search rate and becomes essentially exact for large v . In contrast for a more realistic search rate ($v = 0.1$) the lower panel of Fig. 7 (also discussed in detail later) shows the accuracy of the

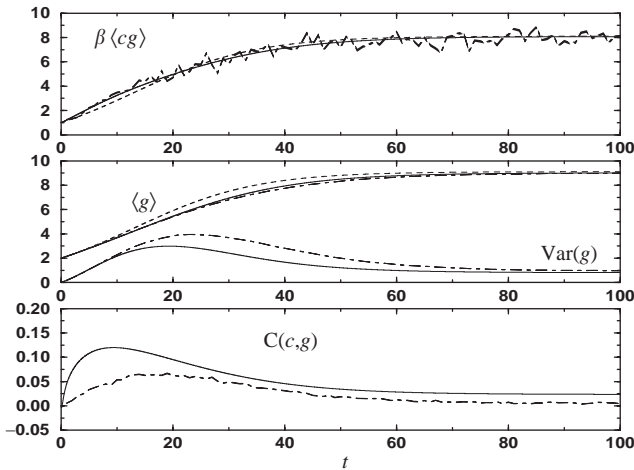


Fig. 3. Moment-closure approximation. The top graph shows the intake rate $\beta \langle cg \rangle$ against time, the middle graph the sward status $\langle g \rangle$ and $\text{Var}(g)$, and the lower graph the association between the animals and the resource in terms of the normalized covariance $C(c, g) = \text{Cov}(c, g) / \sqrt{\text{Var}(g)\text{Var}(c)}$. In each case the solid curves show the log-normal approximation (9)–(14), the dashed curves the non-spatial deterministic model (7), and the dot-dashed curves the results obtained by averaging 200 realizations of the stochastic process simulated on a 10×10 lattice, for 100 evenly spaced time points in the interval $t \in [0, 100]$. The parameter values used are $\beta = 0.1$, $g_0 = 1$, $v = 1$, $\gamma = 0.1$, and $g_{\max} = 10$, with initially uniform sward with $\langle g \rangle = 2$ and with randomly distributed animals at stocking density $\langle c \rangle = 0.1$.

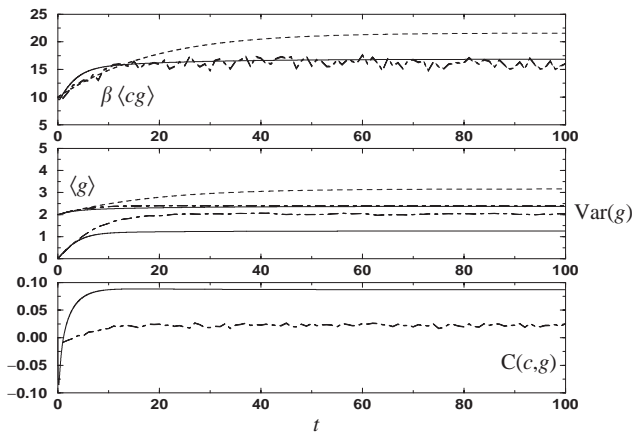


Fig. 4. As Fig. 3, but with $\beta = 1$.

pseudo-spatial model decreasing and then increasing again as the stocking density is increased.

This observed accuracy reflects both the spatial independence (13) and the log-normal (14) assumptions. The latter assumption appears to be reasonable for the distribution of animals across sites, but is a less satisfactory description of sward heights. For example, in the simulations of Fig. 13 the sward height distribution across sites is bimodal for small v , but for large movement rates is well approximated by a log-normal

form (see Fig. 5). The top graph in Fig. 6, which corresponds to the simulations of Fig. 13, shows that nearest neighbour correlations decrease (i.e the accuracy of the spatial approximation (13) increases) as the movement rate increases. Thus the accuracy of both components of the approximation improve with the search rate v . However, for the simulations shown in Fig. 7, at low stocking densities the distribution of sward heights is poorly described by a log-normal, whilst the pseudo-spatial model is rather accurate. In contrast the sward heights have approximately log-normal distributions for intermediate stocking density where the pseudo-spatial model is least accurate. This suggests that the spatial approximations (13) are the key factor determining the accuracy of the pseudo-spatial model. This idea is supported by the results in the lower panel of Fig. 6 which demonstrate that the relative accuracy of the pseudo-spatial model for different stocking densities (shown in Fig. 7) is reflected in the quantity $\langle c(0)g(1) \rangle - \langle c \rangle \langle g \rangle$ which measures the validity of the spatial approximation (13).

These results suggest that the biggest improvement in accuracy of the pseudo-spatial model would come from replacing Eq. (13) with an approximation incorporating between-site correlations. Indeed the importance of accounting for such correlations in spatial models is widely recognized (Rand, 1999). Additional improvement would result from modifying the distributional assumption, for example to account for the bi-modality seen in Fig. 5. Despite these shortcomings we employ the pseudo-spatial log-normal approximation in the remainder of this paper.

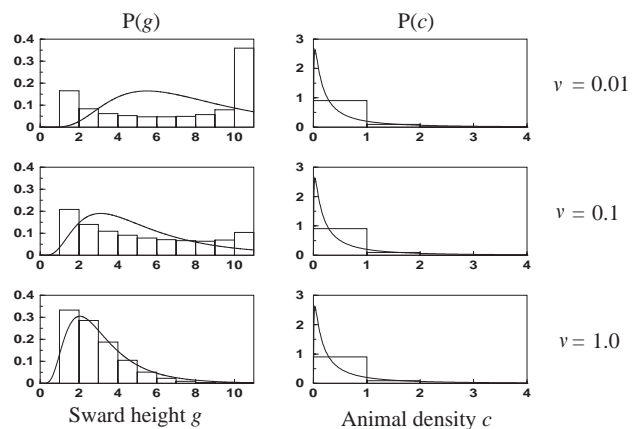


Fig. 5. Validity of distributional assumption. The left-hand graphs compare the sward height distribution $P(g)$ taken from the simulations of Fig. 13 with a log-normal curve for three values of the directed search rate v as shown. The right-hand graphs similarly compare the distribution of animals across sites $P(c)$ taken from the same simulation results. The approximation of $P(c)$ by a log-normal distribution is insensitive to the directed search rate v . In contrast the sward height distribution $P(g)$ becomes increasingly log-normal as v increases.

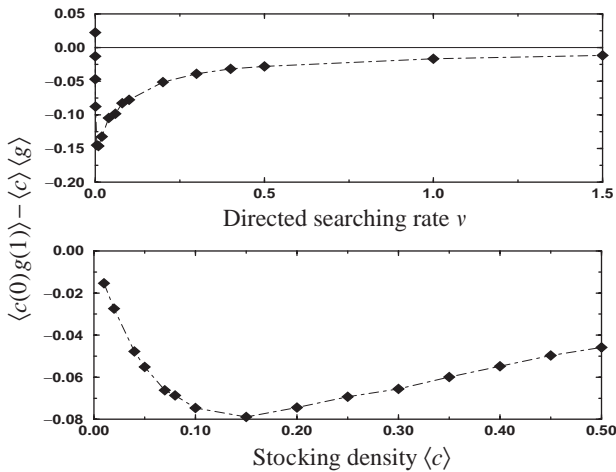


Fig. 6. Validity of spatial independence assumption. Each graph shows $\langle c(0)g(1) \rangle - \langle c \rangle \langle g \rangle$ which measure of the effect of ignoring nearest-neighbour correlations. In the log-normal approximation used in this paper $\langle c(0)g(1) \rangle$ is replaced with $\langle c \rangle \langle g \rangle$ and similar spatial approximations are made for other two-site quantities (see Eq. (13)). The top graph corresponds to the simulations of Fig. 13 and shows that the accuracy of this spatial approximation increases with the directed searching rate. The lower graph shows the validity of such approximations for the simulations shown in Fig. 7 in which the stocking density $\langle c \rangle$ is varied. Comparison with Figures 7 and 13 shows that in each case $\langle c(0)g(1) \rangle - \langle c \rangle \langle g \rangle$ reflects the accuracy of the log-normal approximation.

3.1.2. Spatial heterogeneity and the non-spatial model

Figs. 3 and 4 show not only the log-normal approximation and the spatial stochastic process but also the non-spatial deterministic model (7). The results from the non-spatial model show that spatial effects are relatively minor when the movement rate is large compared with the bite rate. Note that even in this case the pseudo-spatial model is the more accurate and moreover gives a prediction of the spatial heterogeneity ($\text{Var}(g)$ and $C(c, g)$) unavailable from Eq. (7). When $\nu < \beta$ (Fig. 4) the pseudo-spatial model is a considerably more accurate approximation to the stochastic spatial system than the non-spatial deterministic model. In this case comparison of the three models also shows that spatial heterogeneity radically alters both the intake rate $\beta \langle cg \rangle$ and the average sward height $\langle g \rangle$. In the sequel we further explore the role of spatial heterogeneity with reference to animal behaviour and resource management by contrasting the spatial process and its pseudo-spatial approximation with the non-spatial model.

3.2. Optimal resource management

In managing a grazing system there are only a few factors which can be controlled. These include the stocking rate, and perhaps to a lesser extent, the sward quality. Here we wish to consider the impact of spatial heterogeneity on management decisions. We shall focus

on the long-term, or equilibrium, behaviour of the system following any transient phase. Fig. 3 clearly shows both the transient ($t < 50$) and equilibrium ($t > 50$) phases, whilst in Fig. 4 the transient phase is more short-lived. Understanding the equilibrium regime is crucial in the sustainable management of the system. However, we note that the transient phase is also of considerable importance especially in intensively managed systems where human intervention may maintain the system far from equilibrium. In order for the system to reach equilibrium the productivity of the resource must match the total consumption rate of the animals, which corresponds to the criterion that $\beta \langle c \rangle \approx \gamma$. To define the time scale we assume $\beta \approx 1$ and therefore take $\langle c \rangle = \gamma$. In the following we use $N = 100$ patches to model an area which will support $n = 10$ animals, then $\gamma = \langle c \rangle = n/N = 0.1$. As we have seen the relationship between the movement and bite rates is crucial in determining the importance of spatial effects in the system: for $\nu > \beta$ such heterogeneity has a relatively weak effect; whilst for $\nu < \beta$ its role is enhanced. In grass-based systems we expect the bite rate β to be larger than the movement rate ν (WallisDeVries et al., 1998).

Fig. 7 shows the expected average intake rate $\beta \langle cg \rangle$ in the equilibrium regime, for a range of grazing intensities $\beta \langle c \rangle$ for $\nu = 0.2$. The upper graph shows the result of varying the bite rate β , whilst the lower graph shows that of varying the stocking density $\langle c \rangle$. In the non-spatial deterministic model (7) these are equivalent, but in the

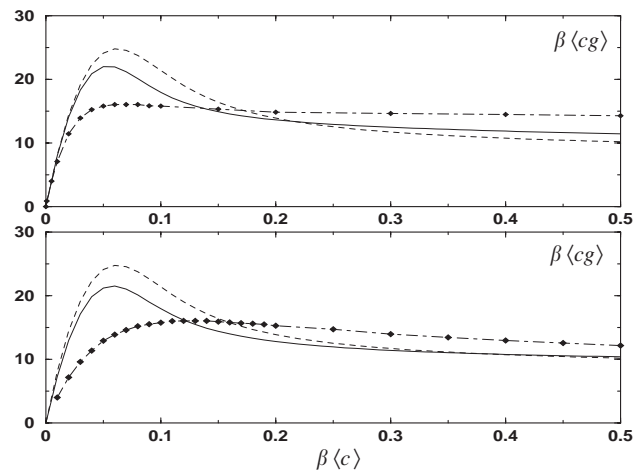


Fig. 7. Optimal stocking density. Both graphs show the intake rate $\beta \langle cg \rangle$ plotted against the grazing intensity $\beta \langle c \rangle$. In the upper graph the grazing rate is varied $\beta \in [0, 5]$ with $\langle c \rangle = 0.1$, whilst in the lower graph the stocking density is varied $\langle c \rangle \in [0, 0.5]$, with $\beta = 1$. In each case the dashed curves show the non-spatial deterministic model (7), the solid curves the log-normal approximation (9)-(14), and the dot-dashed curves with symbols the results obtained by averaging 1000 realizations of the stochastic process simulated on a 10×10 lattice for $t \in [50, 100]$. The size of the symbols represent approximate two standard deviation confidence intervals. The other parameter values used are $g_0 = 1$, $\nu = 0.2$, $\gamma = 0.1$, and $g_{\max} = 10$, with initially uniform sward $\langle g \rangle = 2$ and randomly distributed animals.

log-normal approximation and the spatial stochastic model they are not. In particular, the true optimal stocking density is larger than predicted by either the non-spatial or pseudo-spatial approximations. These results also show that spatial heterogeneity causes a reduction in the productivity of the system, an effect which is captured qualitatively by the log-normal approximation. In particular the optimal stocking density in the spatially heterogeneous system is more than twice that in the non-spatial model, and the corresponding intake rate is found to be approximately 40% lower. Therefore neglecting spatial effects could lead to considerable sub-optimality in resource use. Fig. 8 shows the corresponding results for a larger search rate $\nu = 1.0$, where we find that, although still apparent, the discrepancy between spatial and non-spatial models is reduced, and the accuracy of the log-normal approximation increased.

The model has two measures of resource quality, the growth rate γ , and the maximum sward height g_{\max} . Fig. 9 shows that the expected average intake rate increases with either γ , or g_{\max} . The results suggest that increasing the sward growth rate is a particularly effective way of boosting the intake rate, which rises sharply for small γ . These effects are overestimated by the non-spatial model, and better predicted by the log-normal approximation, particularly for varying g_{\max} .

Spatial heterogeneity therefore has a major impact on issues of resource management. The results presented here suggest that neglecting such effects may lead to an underestimation of the optimal stocking density, and an overestimation of the impact of sward improvement.

3.3. Understanding animal behaviour

3.3.1. Minimum grazable portion

In formulating the spatial grazing process (2) and (6) we assumed that the animals were unable to completely

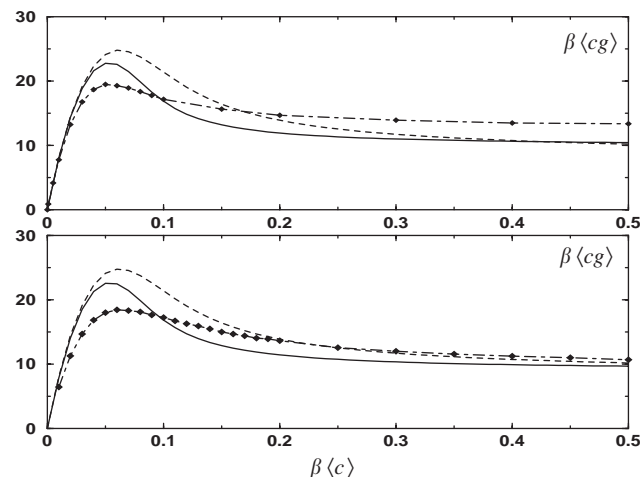


Fig. 8. As Fig. 7, but with larger search rate $\nu = 1.0$.

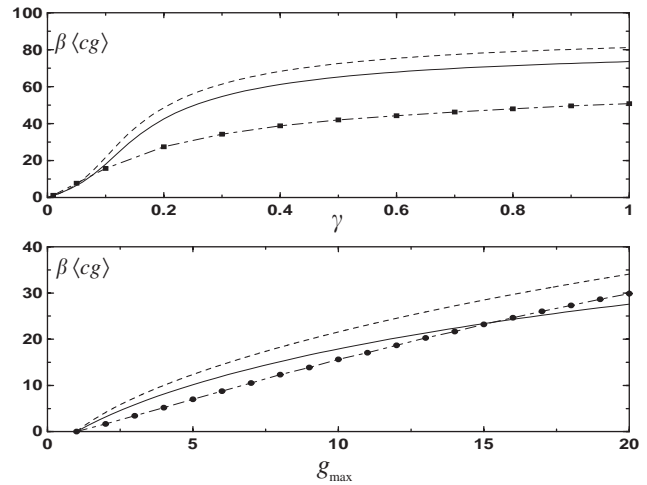


Fig. 9. Resource quality. The top graph shows the intake rate $\beta\langle cg \rangle$ against the sward growth rate $\gamma \in [0, 1]$, and in the lower graph against the maximum sward height $g_{\max} \in [1, 10]$. In each case the dashed curves show the non-spatial deterministic model (7), the solid curves the log-normal approximation (9)–(14), and the dot-dashed curves with symbols the results obtained by averaging 1000 realizations of the stochastic process simulated on a 10×10 lattice for $t \in [50, 100]$. The size of the symbols represent approximate two standard deviation confidence intervals. The parameter values (except for γ and g_{\max} where varied) are $\beta = 1$, $g_0 = 1$, $\nu = 0.2$, $\gamma = 0.1$, and $g_{\max} = 10$, with initially uniform sward $\langle g \rangle = 2$ and randomly distributed animals at stocking density $\langle c \rangle = 0.1$.

deplete the resource due to physical constraints such as bite depth (Flores et al., 1993; Laca et al., 1992; Ungar and Ravid, 1999), and this was described in terms of the minimum grazable portion g_0 . However, is there some advantage in raising g_0 above this physical limit—for example to allow for faster re-growth? The results of Fig. 10, which shows an optimal intake rate for $g_0 \approx 2$, suggests that there might. This observation is consistent with grazing systems in which bite mass values leave a residual leaf area index to optimize re-growth (Caldwell et al., 1981; Jatimlinsky et al., 1997; Johnson and Thornley, 1984; Schapendonk et al., 1998; Warringa and Kreuzer, 1996). Note also that once again ignoring spatial effects alters the results, with the non-spatial model predicting a larger optimal g_0 . Pasture managers might be able to manipulate g_0 via breeding programmes and in any case it is likely that it has been optimized by natural selection. However, it should be emphasized that an optimal g_0 arising from our model must be treated with caution in the context of natural selection as no account has been taken of between animal competition and there is no advantage in leaving resources for a competitor to consume.

3.3.2. The impact of searching behaviour

An interesting question is whether directed searching is more efficient than a random searching strategy. Alternatively what impact does the inclusion of the more

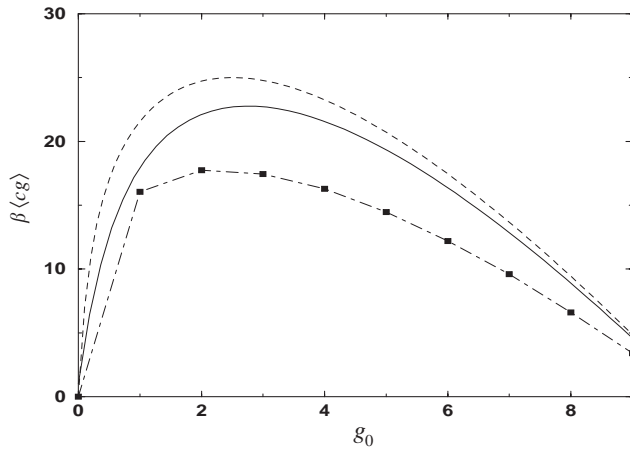


Fig. 10. Optimal minimum grazable portion. The intake rate $\beta\langle cg \rangle$ is plotted against the minimum grazable portion g_0 . The dashed curves show the non-spatial deterministic model (7), the solid curves the log-normal approximation (9)–(14), and the dot-dashed curves with squares the results obtained by averaging 1000 realizations of the stochastic process simulated on a 10×10 lattice for $t \in [50, 100]$. The size of the squares represents approximate two standard deviation confidence intervals. The parameter values used are $\beta = 1$, $g_0 \in [0, 9]$, $v = 0.2$, $\gamma = 0.1$, and $g_{\max} = 10$, with initially uniform sward $\langle g \rangle = 2$ and randomly distributed animals at stocking density $\langle c \rangle = 0.1$.

realistic directed searching behaviour have on the system? To address such questions, modify the search rate to include random movement of an individual at site i to some neighbouring site $j \in \mathcal{N}_i$ at rate v_{rnd}/z . Eq. (6) is therefore modified to

$$\begin{array}{rcccl}
 R(n \rightarrow n + \delta n) & \delta g_i & \delta c_i & \delta c_j & \\
 \gamma g_i(1 - g_i/g_{\max}) & +1 & 0 & 0 & \text{Growth at } i, \\
 \beta c_i(g_i - g_0) & -1 & 0 & 0 & \text{Bite at } i, \\
 \frac{z}{z}(v_{\text{rnd}} + v g_j) & 0 & -1 & +1 & \text{Move } i \rightarrow j \in \mathcal{N}_i
 \end{array} \tag{15}$$

and Eqs. (2) and (15) define a new model including both random and directed local searching. Moment-equations can be derived, indeed the only change is the addition of the term $2v_{\text{rnd}}z$ to Eq. (12), and a log-Normal closure scheme applied as before. Fig. 11 shows a comparison of random only, and directed only searching over time. The search rates $v_{\text{rnd}} = 1.0$ and $v = 0.2$ have been chosen so that the resultant rates of movement are lower for the more targeted search. Note that the random movement rate v_{rnd} appears larger as it is not scaled by the local sward height in Eq. (15). The results show that directed searching is more efficient than the random strategy, requiring less moves per unit time to achieve a greater intake rate $\beta\langle cg \rangle$. Note that the movement rate for the random search model is essentially constant over time whilst the movement rates in the directed search model increase to an asymptote. This behaviour is understood by reference to Fig. 12 which shows the sward heterogeneity $\text{Var}(g)$ increasing over

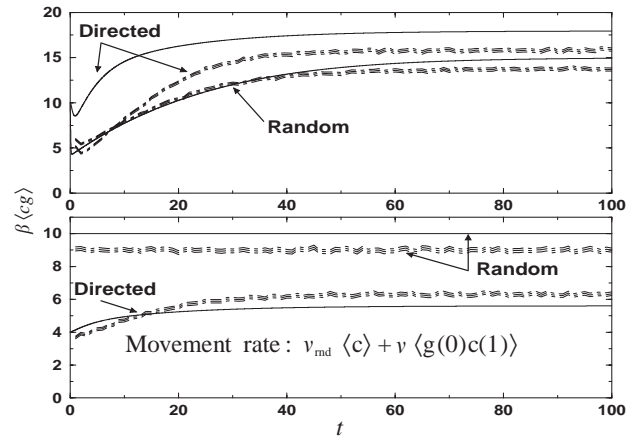


Fig. 11. Random and directed searching. The top graph shows the intake rate $\beta\langle cg \rangle$ and the lower the movement rate $v_{\text{rnd}}\langle c \rangle + v\langle g(0)c(1) \rangle$, both plotted against time t . In each graph results are shown for random ($v_{\text{rnd}} = 1.0$, $v = 0$) and directed searching ($v_{\text{rnd}} = 0$, $v = 0.2$) as indicated. Simulation results are shown by the dot-dashed curves and log-normal approximations by the solid curves. The simulation results were obtained by averaging 10000 realizations of the stochastic process simulated on a 10×10 lattice for 100 evenly spaced time points in the interval $[0, 100]$, and two standard deviation confidence intervals are shown. The other parameter values are $\beta = 1$, $g_0 = 1$, $\gamma = 0.1$, and $g_{\max} = 10$, with initially uniform sward $\langle g \rangle = 2$ and randomly distributed animals at stocking density $\langle c \rangle = 0.1$.

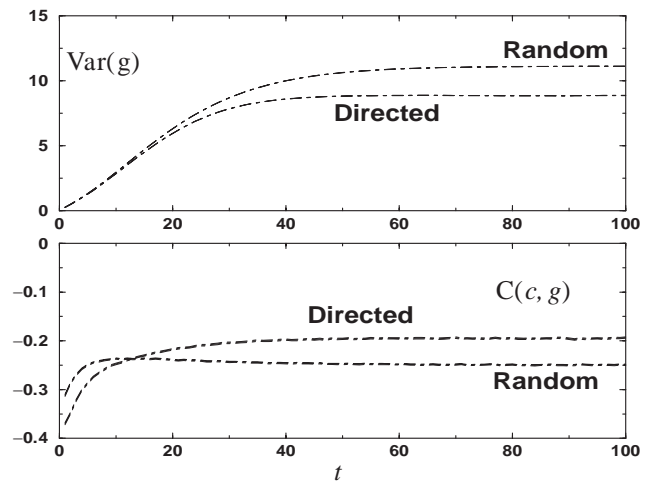


Fig. 12. Sward heterogeneity and the association between foragers and the resource. The top graph shows the variance $\text{Var}(g)$ against time t , whilst the lower plots the association between animal and sward $C(c, g)$ obtained from the simulations shown in Fig. 11. The results for random ($v_{\text{rnd}} = 1.0$, $v = 0$) and directed ($v_{\text{rnd}} = 0$, $v = 0.2$) searching are indicated by the labels Random and Directed, respectively.

the same period. The sward is initially uniform and therefore the number of moves required by directed searching is minimal. However, as time goes on the spatial heterogeneity of the resource grows and there is a commensurate increase in directed searching. In contrast random searching is insensitive to the resource

distribution. In addition, Fig. 12 shows that directed searching ultimately results in a reduced level of sward heterogeneity when compared with random searching. Moreover, as expected the correlation between the animals and the resource is greater for directed searching once the sward develops sufficient heterogeneity.

Fig. 13 shows the expected equilibrium intake rates associated with random searching and directed search for a wide range of movement rates associated with $v \in [0, 5]$ and $v_{\text{rnd}} \in [0, 11]$. The advantage of directed over random searching (per move) is most marked when the search rate v is smaller, or comparable with the bite rate β . As noted earlier this is a characteristic of grazing systems. For larger search rates this advantage is considerably reduced and, for a directed search rate which is approximately twice the bite rate, the random strategy maximizes the expected equilibrium intake rate. The log-normal approximation, shown for the directed search model, is again increasingly accurate as the search rate increases. That a random search method should out-perform directed searching for large search rates seems puzzling until one notes that, over the long term, each behaviour modifies the environment, in this case the sward height and distribution. The lower graph of Fig. 13 shows the average sward heights in equilibrium. The long term effect of directed searching

is a much shorter sward than that associated with random searching. Thus, animal behaviour has a major impact on the environment, with the more efficient strategy (on short time scales) depleting the sward to a greater extent. Despite this lower average sward height directed searching is able to out do random searching for a wide range of search rates.

Although the directed search strategy considered here only accounts for resource selection in a rather crude way, the random search may be regarded as essentially behaviour free. In this section we have found that incorporation of behaviour via simple rules of thumb, such as directed searching, can radically alter model predictions (See e.g. Figs 11 and 13). In particular, for foraging animals it is the interaction between individual behaviour and a spatially heterogeneous environment which accounts for these differences. Schwinning and Parsons (1999) use a counter example to point out that the widely held view that sward heterogeneity is always deleterious to production is not correct. However, in Fig. 11, the inclusion of more realistic animal behaviour suggests that greater search effort is required as sward heterogeneity increases. In addition our results show that patch selection can simultaneously increase intake and drive down sward heterogeneity when compared with random selection (Figs. 11 and 12).

3.3.3. Avoided areas

A key feature of foraging behaviour in grazing animals is that of avoidance, the canonical example of which is faecal avoidance (Bao et al., 1998; Cooper et al., 2000). Animals can only detect the presence of faeces locally through olfactory stimuli, and therefore an individual may travel to a promising patch only to find it contaminated. For a high level of contamination and a marked aversion to faeces this behaviour will reduce the animals intake rate. Since contaminated patches are more likely to be ungrazed they will be taller than the average patch, with potentially detrimental effects on searching efficiency. Similar considerations apply to any unpalatable characteristic which is only detected locally, for example in mixed swards the presence of an unpalatable species hidden (at a distance) within a stand of a more preferred species. Nonetheless here we will focus on faecal avoidance.

Faecal deposition is a major source of heterogeneity in grazing systems (Hutchings et al., 2001, 2002a,b). The deposition of faeces is often non-random with concentrations tending to accumulate at specific sites (Haynes and Williams, 1993). Herbivores avoid grazing swards contaminated with faeces and thus parasites: fresh faeces are avoided most strongly and this avoidance declines with the age of faeces (Hutchings et al., 1998). During the initial period of faecal avoidance the surrounding sward may become relatively tall, creating patches of tall sward (Hutchings et al., 2001). Also, as a consequence of

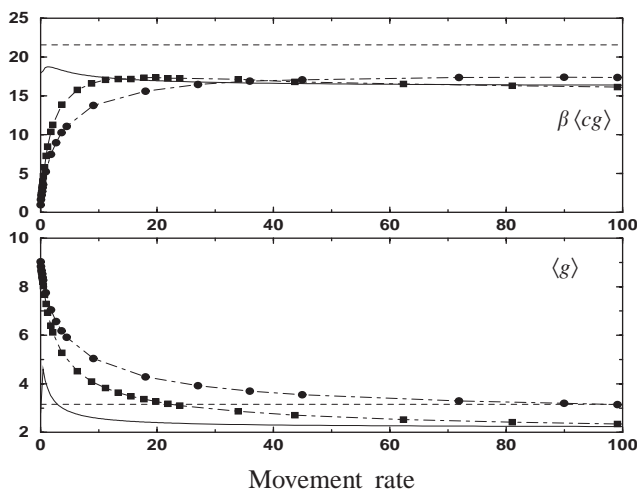


Fig. 13. Random and directed searching. The top graph shows the expectation of the intake rate, $\beta \langle cg \rangle$ against the movement rate, whilst the lower graphs plots the corresponding average sward height $\langle g \rangle$. In each graph simulation results for random searching ($v_{\text{rnd}} \in [0, 11]$, $v = 0$) are shown by the circular symbols, and for directed searching ($v_{\text{rnd}} = 0$, $v \in [0, 5]$) by squares. For the directed search model only the results from the non-spatial deterministic model (7) are shown by the dashed curves whilst those of the log-normal approximation (9)–(14) are shown by solid curves. The simulation results were obtained by averaging 1000 realizations of the stochastic process on a 10×10 lattice for $t \in [50, 100]$, and two standard deviation confidence intervals are smaller than the symbol size. The other parameter values are $\beta = 1$, $g_0 = 1$, $\gamma = 0.1$, and $g_{\text{max}} = 10$, with initially uniform sward $\langle g \rangle = 2$ and randomly distributed animals at stocking density $\langle c \rangle = 0.1$.

the concentrating effect of digestion and defecation there tend to be high levels of nutrients (nitrogen, phosphorus and potassium) in areas of faecal deposits. This has an important effect on nutrient cycling and in low nutrient ecosystems, typical of many extensive rangelands, can lead to an increase in soil nutrient levels around defecations. Consequently, the plants associated with areas where faeces are concentrated tend to have higher concentrations of nutrients in their tissues than the average in the system (Edwards and Hollis, 1982). This faeces avoidance behaviour may then be seen as leading to a mosaic of tall, nutrient rich and short, nutrient poor sward patches (Penning et al., 1991; Gordon et al., 1996; Hutchings et al., 2001). The increased sward height and nutrient concentration of swards associated with faeces makes them highly desirable for grazing.

To explore these issues we introduce faecal contamination, avoidance behaviour and the fertilization effect into our model. Faecal contamination is f_i in patch i and is assumed to be randomly distributed at rate $\langle f \rangle$. In reality faeces is deposited by the foragers and then decays over time. However, here it is assumed that the faeces does not decay but remains fixed at the initial value. Thus we can explore the impact of varying levels of contamination without considering the complication of faecal deposition and decay. The local avoidance of faecally contaminated patches is introduced by multiplying the bite rate by an exponential function of the contamination level $\exp(-\mu f_i)$, where the parameter μ represents the strength of the avoidance behaviour. Thus, the avoidance behaviour intensifies with increasing μ and faecal contamination f_i . The fertilizer effect simply inflates the growth rate at site i by an amount linearly dependent on f_i and controlled by the parameter γ_{fc} . Eq. (6) is therefore modified to

$R(n \rightarrow n + \delta n)$	δg_i	δc_i	δc_j	
$\gamma(1 + \gamma_{fc} f_i) g_i (1 - g_i / g_{max})$	+1	0	0	Growth at i
$\beta c_i (g_i - g_0) e^{-\mu f_i}$	-1	0	0	Bite at i
$\frac{c_i}{z} (v_{rnd} + v g_j)$	0	-1	+1	Move
				$i \rightarrow j \in \mathcal{N}_i$

(16)

and Eqs. (2) and (16) define a faecal avoidance model. Fig. 14 shows some results from this model for both directed and random searching. At a fixed level of contamination the intake rate decreases with increasing faecal avoidance μ . For a given μ the decrease in intake compared with $\mu = 0$ represents the trade-off associated with avoidance behaviour. For $\mu \approx 5$ the animals almost completely avoid contaminated patches. Moreover, the effect is similar for both search strategies, although as anticipated there is a slight reduction in the relative efficiency of directed searching. Fig. 14 shows trade-off

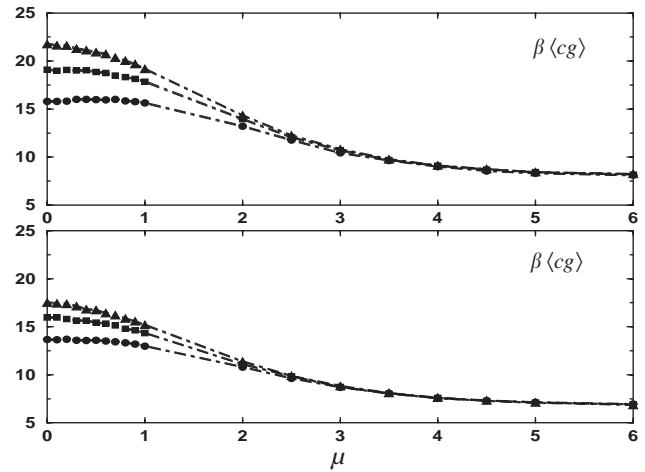


Fig. 14. Effect of faecal avoidance. The intake rate, $\beta \langle cg \rangle$ is plotted against degree of avoidance μ for the faecal avoidance model (16) for the directed (upper graph) and random (lower graph) searching rates used in Fig. 11. In each graph the curves correspond to different levels of the fertilizer effect is $\gamma_{fc} = 0.0$ (circles), $\gamma_{fc} = 0.5$ (squares), $\gamma_{fc} = 1.0$ (triangles). The results were obtained from simulation by averaging 1000 realizations of the stochastic process on a 10×10 lattice for $t \in [50, 100]$. The size of the symbols represent approximate two standard deviation confidence intervals. The parameter values are $\beta = 1$, $g_0 = 1$, $\gamma = 0.1$, and $g_{max} = 10$, $\langle f \rangle = 0.5$, with initially uniform sward $\langle g \rangle = 2$ and randomly distributed animals at stocking density $\langle c \rangle = 0.1$.

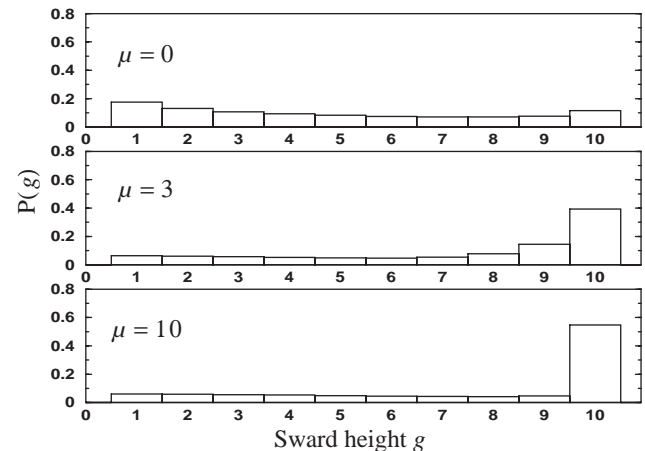


Fig. 15. Effect of faecal avoidance on sward structure. Histograms of the sward height across patches obtained from the simulations shown in Fig. 14 for $\gamma_{fc} = 0.5$ and low, intermediate and high levels of faecal avoidance μ as indicated.

curves corresponding to high ($\gamma_{fc} = 0$), medium ($\gamma_{fc} = 0.5$) and low ($\gamma_{fc} = 1$) nutrient soils. In the nutrient poor system faecal contamination provides scarce resources, sward growth is greatly enhanced, and the penalty paid for faecal avoidance is proportionately higher.

Fig. 15 shows the impact of avoidance behaviour on the structure of the sward for directed searching. When the foragers do not avoid contaminated patches the

sward is relatively uniform. However, as avoidance behaviour becomes more pronounced the sward becomes increasingly heterogeneous, with lightly grazed contaminated areas growing taller than their uncontaminated and more heavily grazed counterparts.

4. Discussion

We have developed a simple spatial and stochastic model of foraging. The model focuses on the behaviour of individuals foraging in an extended spatial domain, but whose knowledge is limited to their own local neighbourhood. It is assumed that, within this neighbourhood animals are able to assess the quality of the resources and move preferentially towards the best available (e.g. grazing animals move towards tall swards). However, individuals can only assess secondary, harmful or otherwise undesirable, characteristics at their current location (e.g. olfactory assessment of local faecal contamination). Mobility plays a key role; for small search rates, v , spatial heterogeneity radically alters the productivity of the system, whereas for large search rates such effects are minimized. Approximations to the stochastic spatial system were constructed by considering the evolution of the moments of the process. The simplest approximation, which corresponds to neglecting the variance–covariance structure is equivalent to the non-spatial deterministic model, whilst the second-order, log-normal, approximation may be considered to be a pseudo-spatial model as it accounts for some of the heterogeneity seen in the fully spatial model. The discrepancy between the three models grows, with spatial heterogeneity, as the search rate v decreases. Detailed comparison of the pseudo-spatial approximation with simulations shows that it could be improved primarily by accounting for between-site correlations, but also by employing more appropriate (bimodal) distributional assumptions. These challenges remain the subject of future work.

Our results show that spatial heterogeneity radically alters the sustainable optimal stocking density of the system, with the non-spatial model simultaneously under-estimating the optimal stocking rate and over-estimating the corresponding yield. Similar although less striking differences were found when considering changes in the productivity of the sward. Three aspects of animal behaviour were explored: the minimum grazable portion; search strategies; and faecal avoidance. Perhaps the most important conclusion is that incorporating realistic behavioural characteristics has a profound impact on model output. Firstly, this is true of the minimum grazable portion, the optimal value of which is altered by spatial heterogeneity. Secondly, for a given movement rate and resource distribution directed searching resulted in a higher intake rate than a random

strategy. Moreover, using directed searching individuals are able to respond dynamically to changes in the resource distribution, increasing search rates in more heterogeneous environments. Thirdly, in contaminated pastures faecal avoidance behaviour causes a reduction in the intake rate. This trade-off increases with the degree of avoidance and is greater in nutrient-poor than nutrient-rich systems. Interestingly, however, despite the correlation between contamination and tall swards the trade-off does not tip the balance in favour of random searching.

A key issue not directly addressed in this paper is that of scale. What patch size is appropriate to model foraging behaviour? Clearly this will depend on the system under study and the questions one seeks to answer. For example, in the context of dairy grazing the patch size could be set with reference to the typical area affected by faecal contamination $\approx 0.5 \text{ m}^2$. This leads to approximately 20000 patches per hectare, which is rather computationally demanding. However, as noted earlier preliminary results not reported here in detail suggest that the broad conclusions drawn in the present paper are remarkably robust to changes in patch scale. Moreover, in such situations the pseudo-spatial model may provide a good compromise between computational tractability and realism. Such a compromise may also be appropriate if models of foraging behaviour were required on a landscape scale.

In the present paper we have largely focused on grazing behaviour, but the modelling framework developed here is sufficiently flexible to be relevant to other foraging systems. For example, it was argued that in the grazing context movement rates v should be lower than the bite rate β , however in systems where the resource is scarce, but of higher value it is expected that $v > \beta$, for which spatial heterogeneity will be less significant. Indeed in such cases the pseudo-spatial approximation should prove to be highly accurate. Nonetheless application of our model to a more general foraging contexts may require modifications such as accounting for the costs of searching.

The modelling framework introduced here allows further layers of behavioural complexity and other features to be added. These could include: animal behaviour modified by the physiological state of the individual, for example current nutritional or lactating status; defecation; decay of faeces; interaction between animals; and spatio-temporal variation in sward characteristics reflecting underlying environmental heterogeneities. However, the sward growth model and the simple description of behaviour, adopted in this paper, seem to capture at a very basic level the plant–animal interaction in grazing systems. Moreover, our approach demonstrates the key importance of individual behaviour in response to local knowledge in spatially heterogeneous environments.

Acknowledgements

BioSS and SAC receive support from the Scottish Executive Environment and Rural Affairs Department (SEERAD). MRH receives support from a SEERAD Senior Research Fellowship.

Appendix A. Moment evolution equations and log-normal approximation

Here we show how to obtain moment equations for the spatio-temporal Markov processes considered in this paper. In particular we start by deriving Eq. (5) from the definition of the global directed search model (2) and (3).

A.1. Global directed search model

Write the change in the sward height at site i during the interval $(t, t + \delta t)$ as $g_i(t + \delta t) - g_i(t) = \delta g_i(t)$. Since the random variable $\delta g_i(t)$ is defined by Eqs. (2) and (3) then taking the expectation at time $t + \delta t$ conditional on the state of the system at time t yields

$$E[g_i(t + \delta t) | n(t)] - g_i(t) = (+1)\gamma g_i \delta t + (-1)\beta c_i g_i \delta t + O(\delta t^2).$$

Note that multiple events may be ignored as they occur with probability of order $O(\delta t^2)$. Now taking expectations at time t and summing over $i = 1, \dots, N$ leads to

$$E \left[\sum_{i=1}^N g_i(t + \delta t) \right] - E \left[\sum_{i=1}^N g_i(t) \right] = \gamma E \left[\sum_{i=1}^N g_i \right] \delta t - \beta E \left[\sum_{i=1}^N c_i g_i \right] \delta t + O(\delta t^2).$$

Finally dividing by $N\delta t$ and taking the limit as $\delta t \rightarrow 0$ we obtain

$$\frac{d}{dt} \langle g \rangle = \gamma \langle g \rangle - \beta \langle cg \rangle,$$

where we have used the angle brackets $\langle \cdot \rangle$ to denote the expectation of the spatial average, defined by Eq. (4). Eq. (5) then follows upon noting that the second-order term may be decomposed as $\langle cg \rangle = \langle c \rangle \langle g \rangle + \text{Cov}(c, g)$. In a similar vain we may consider the change in c_i to obtain

$$E \left[\sum_{i=1}^N c_i(t + \delta t) \right] - E \left[\sum_{i=1}^N c_i(t) \right] = E \left[v \sum_{j=1}^N c_j \sum_{i=1}^N g_i - v \sum_{i=1}^N c_i \sum_{j=1}^N g_j \right] \delta t.$$

Noting that the right-hand side is zero, dividing by $N\delta t$ and taking the limit as $\delta t \rightarrow 0$ we obtain

$$\frac{d}{dt} \langle c \rangle = 0.$$

A.2. Local directed search model

Focusing on the local directed search model the equation for the conditional expectation of the change in g_i during a time interval $(t, t + \delta t)$, is

$$E[g_i(t + \delta t) | n(t)] - g_i(t) = (+1)\gamma g_i(t)(1 - g_i/g_{\max})\delta t + (-1)\beta c_i(t)(g_i(t) - g_0)\delta t.$$

Note that this result follows from the model definition (2) and (6). In this case, following the steps outlined above leads to:

$$\frac{d}{dt} \langle g \rangle = \gamma \left(\langle g \rangle - \frac{\langle g^2 \rangle}{g_{\max}} \right) - \beta (\langle cg \rangle - g_0 \langle c \rangle).$$

Whence on applying the definitions $\text{Var}(g) = \langle g^2 \rangle - \langle g \rangle^2$ and $\text{Cov}(c, g) = \langle cg \rangle - \langle c \rangle \langle g \rangle$ one obtains Eq. (9). The equation for the evolution of the expected average animal density $\langle c \rangle$ is similar to that obtained above for the global directed search model except that the summations over j , rather than being over the entire lattice, are now over the sites in the neighbourhood \mathcal{N}_i of site i , thus

$$E \left[\sum_{i=1}^N c_i(t + \delta t) \right] - E \left[\sum_{i=1}^N c_i(t) \right] = E \left[v \sum_{j \in \mathcal{N}_i} c_j \sum_{i=1}^N g_i - v \sum_{i=1}^N c_i \sum_{j \in \mathcal{N}_i} g_j \right] \delta t.$$

Dividing by $N\delta t$ and taking the limit as $\delta t \rightarrow 0$ yields

$$\frac{d}{dt} \langle c \rangle = zv(\langle c(0)g(1) \rangle - \langle g(0)c(1) \rangle),$$

where

$$z \langle c(0)g(1) \rangle = E \left[\frac{1}{N} \sum_{i=1}^N c_i \sum_{j \in \mathcal{N}_i} g_j \right]$$

with the analogous definition of $\langle g(0)c(1) \rangle$. Since both quantities measure the correlation between the sward height at a given site and the animal density in its neighbouring sites (i.e. only the relative positions are relevant) then $\langle g(0)c(1) \rangle = \langle c(0)g(1) \rangle$ and it follows that $d\langle c \rangle/dt = 0$.

Calculation of the second-order statistics proceeds in a similar manner to that of the first-order terms. Rearrange the equation $c_i(t + \delta t)g_i(t + \delta t) = (c_i(t) + \delta c_i(t))(g_i(t) + \delta g_i(t))$ to obtain the change in $c_i g_i$

over the interval $(t, t + \delta t)$,

$$c_i(t + \delta t)g_i(t + \delta t) - c_i(t)g_i(t) = c_i\delta g_i + g_i\delta c_i + \delta c_i\delta g_i.$$

Note that the left-hand side is to be evaluated at time t . From Eqs. (2) and (6) the expectation of this expression conditional on the state of the system at time t is

$$\begin{aligned} & E[c_i(t + \delta t)g_i(t + \delta t) | n(t)] - c_i(t)g_i(t) \\ &= g_i \left((+1)^v \sum_{j \in \mathcal{N}_i} c_j g_i + (-1)^v \sum_{j \in \mathcal{N}_i} c_i g_j \right) \delta t \\ &+ c_i \left((+1)^v \gamma g_i \left(1 - \frac{g_i}{g_{\max}} \right) + (-1)^v \beta c_i (g_i - g_0) \right) \\ &\times \delta t + O(\delta t^2). \end{aligned}$$

The term $\delta c_i\delta g_i$ makes an $O(\delta t^2)$ contribution since no single event simultaneously changes the sward height and the animal density. As before we now take expectations at time t , sum over $i = 1, \dots, N$, divide by $N\delta t$ and take the limit as $\delta t \rightarrow 0$. This procedure leads to

$$\begin{aligned} \frac{d}{dt} \langle cg \rangle &= vz(\langle g(0)g(0)c(1) \rangle - \langle c(0)g(0)g(1) \rangle) \\ &+ \gamma(\langle cg \rangle - \frac{\langle cg^2 \rangle}{g_{\max}}) \\ &- \beta(\langle c^2g \rangle - \langle c^2 \rangle g_0), \end{aligned}$$

where the two-site terms are defined by

$$\begin{aligned} \langle g(0)g(0)c(1) \rangle &= \frac{1}{z} E \left[\frac{1}{N} \sum_{i=1}^N g_i g_i \sum_{j \in \mathcal{N}_i} c_j \right] \text{ and} \\ &\times \langle c(0)g(0)g(1) \rangle \\ &= \frac{1}{z} E \left[\frac{1}{N} \sum_{i=1}^N c_i g_i \sum_{j \in \mathcal{N}_i} g_j \right]. \end{aligned}$$

Employing the definitions for $\text{Cov}(c, g)$, $\text{Var}(g)$ and $\text{Var}(c) = \langle c^2 \rangle - \langle c \rangle^2$ and noting that $d\text{Cov}(c, g)/dt = d\langle cg \rangle/dt - \langle c \rangle d\langle g \rangle/dt - \langle g \rangle d\langle c \rangle/dt$ finally yields Eq. (10). The derivations of Eqs. (11) and (12) follow a similar path starting from $g_i^2(t + \delta t) = (g_i(t) + \delta g_i(t))^2$, and $c_i^2(t + \delta t) = (c_i(t) + \delta c_i(t))^2$, respectively.

A.3. Log-normal approximation

If the sward height g_i and animal numbers c_i are log-normally distributed over space and time (Keeling et al., 2000), then $y_1 = \log c_i$ and $y_2 = \log g_i$ are joint Normal with m.g.f. (Kendall, 1994)

$$\begin{aligned} M(\theta_1, \theta_2) &\equiv \langle \exp\{\theta_1 y_1 + \theta_2 y_2\} \rangle \\ &= \exp\{\kappa_{10}\theta_1 + \kappa_{01}\theta_2 + \kappa_{20}\theta_1^2/2 \\ &+ \kappa_{11}\theta_1\theta_2 + \kappa_{02}\theta_2^2/2\}, \end{aligned}$$

where $\langle \cdot \rangle$ denotes the expectation over distributions in space and time, and

$$\begin{aligned} \kappa_{10} &= 2 \log(\langle c \rangle) - \log(\langle c^2 \rangle)/2, \\ \kappa_{01} &= 2 \log(\langle g \rangle) - \log(\langle g^2 \rangle)/2 \\ \kappa_{20} &= \log(\langle c^2 \rangle) - 2 \log(\langle c \rangle), \\ \kappa_{02} &= \log(\langle g^2 \rangle) - 2 \log(\langle g \rangle), \\ \kappa_{11} &= \log(\langle cg \rangle) - (\kappa_{20} + \kappa_{02})/2 - \kappa_{10} - \kappa_{01}. \end{aligned}$$

For appropriate choice of θ_1 and θ_2 the approximations (14) of the higher-order terms $\langle c^2g \rangle$, $\langle cg^2 \rangle$ and $\langle g^3 \rangle$ are obtained from

$$\langle c^{\theta_1} g^{\theta_2} \rangle = \langle \exp\{\theta_1 y_1 + \theta_2 y_2\} \rangle = M(\theta_1, \theta_2).$$

For example setting $\theta_1 = 2$ and $\theta_2 = 1$ yields

$$\begin{aligned} \langle c^2g \rangle &= M(2, 1) \\ &= \exp\{2\kappa_{10} + \kappa_{01} + 2\kappa_{20} + 2\kappa_{11} + \kappa_{02}/2\}, \end{aligned}$$

which simplifies to

$$\langle c^2g \rangle = \frac{\langle c^2 \rangle \langle cg \rangle^2}{\langle c \rangle^2 \langle g \rangle}.$$

References

- Arnold, G.E., 1987. Influence of the biomass, botanical composition and sward height of annual pastures on foraging behaviour of sheep. *J. Appl. Ecol.* 24, 759–772.
- Bao, J., Giller, P.S., Stakelum, G., 1998. Selective grazing by dairy cows in the presence of dung and the defoliation of tall grass dung patches. *Science* 66, 65–73.
- Bazely, D.R., 1990. Rules and cues used by sheep foraging in monocultures. In: Hughes, R.N. (Ed.), *Behavioural Mechanisms of Food Selection*. Springer, London, pp. 343–367.
- Bazely, D.R., Ensor, C.V., 1989. Discrimination learning in sheep with cues varying in brightness and hue. *Appl. Anim. Behav. Sci.* 23, 293–299.
- Black, J.L., Kenney, P.A., 1984. Factors affecting diet selection by sheep. ii height and density of pasture. *Aust. J. Agr. Res.* 35, 565–578.
- Bolker, B., Pacala, S.W., 1997. Using moment equations to understand stochastically driven pattern formation in ecological systems. *Theor. Popul. Biol.* 52, 179–197.
- Caldwell, M.M., Richards, J.H., Johnson, D.A., Nowak, R.S., Dzuree, R.S., 1981. Coping with herbivory: Photosynthetic capacity and resource allocation in two semiarid agropyron bunchgrasses. *Oecologia* 50, 14–24.
- Carrere, P., Louault, F., De Faccio Carvalho, P.C., Lafarge, M., Soussana, J.F., 2001. How does the vertical and horizontal structure of a perennial ryegrass and white clover sward influence grazing? *Grass Forage Sci.* 56, 118–130.
- Cazcarra, R.F., Petit, M., 1995. The influence of animal age and sward height on the herbage intake and grazing behavior of Charolais cattle. *Anim. Sci.* 61, 497–506.
- Cooper, J., Gordon, I.J., Pike, A.W., 2000. Strategies for the avoidance of faeces by grazing sheep. *Appl. Anim. Behav. Sci.* 69, 15–33.
- Cox, D.R., Miller, H.D., 1965. *The Theory of Stochastic Processes*. Chapman & Hall, London.

- Dohi, H., Yamada, A., Entsu, S., 1991. Cattle feeding deterrents emitted from cattle faeces. *J. Chem. Ecol.* 17, 1197–1203.
- Edwards, P.J., Hollis, S., 1982. The distribution of excreta on new forest grassland used by cattle, ponies and deer. *J. Appl. Ecol.* 19, 953–964.
- Ferguson, N.M., Donnelly, C.A., Anderson, R.M., 2001. The foot and mouth epidemic in Great Britain: Pattern of spread and impact of interventions. *Science* 292, 1155–1160.
- Filipe, J.A.N., Gibson, G.J., 1998. Studying and approximating spatio-temporal models for epidemic spread and control. *Philos. Trans. R. Soc. London B* 353, 2153–2162.
- Flores, E.R., Laca, E.A., Griggs, T.C., Demment, M.W., 1993. Sward height and vertical morphological-differentiation determine cattle bite dimensions. *Agron. J.* 85, 527–532.
- Fryxell, J.M., 1991. Forage quality and aggregation by large herbivores. *Am. Nat.* 138, 478–498.
- Gibb, M.J., Huckle, C.A., Nuthall, R., 1998. Effect of time of day on grazing behaviour by lactating dairy cows. *Grass Forage Sci.* 53, 41–46.
- Gibb, M.J., Huckle, C.A., Nuthall, R., 2002. Effects of level of concentrate supplementation on grazing behaviour and performance by lactating dairy cows grazing continuously stocked grass swards. *Anim. Sci.* 74, 319–335.
- Gordon, I.J., Illius, A.W., Milne, J.D., 1996. Sources of variation in the foraging efficiency of grazing ruminants. *Funct. Ecol.* 10, 219–226.
- Grunbaum, D., 1998. Using spatially explicit models to characterize foraging performance in heterogeneous landscapes. *Am. Nat.* 151, 97–115.
- Haynes, R.J., Williams, P.H., 1993. Nutrient cycling and soil fertility in the grazed pasture ecosystem. *Adv. Agron.* 49, 119–199.
- Hodgson, J., Illius, A.W., 1996. *The Ecology and Management of Grazing Systems*. CAB International, Oxford.
- Hutchings, M.R., Kyriazakis, I., Anderson, D.H., Gordon, I.J., Coop, R.L., 1998. Behavioural strategies used by parasitised and non-parasitised sheep to avoid ingestion of gastrointestinal nematodes. *Anim. Sci.* 67, 97–106.
- Hutchings, M.R., Gordon, I.J., Kyriazakis, I., Jackson, F., 2001. Herbivore avoidance of faeces-contaminated patches leads to a trade-off between intake rate of forage and parasitism in subsequent foraging decisions. *Anim. Behav.* 62, 955–964.
- Hutchings, M.R., Gordon, I.J., Kyriazakis, I., Robertson, E., Jackson, F., 2002a. Grazing in heterogeneous environments: Infra and supra-parasite distributions determine herbivore grazing decisions. *Oecologia* 132, 453–460.
- Hutchings, M.R., Milner, J.M., Gordon, I.J., Kyriazakis, I., Jackson, F., 2002b. Grazing decisions of Soay sheep (*Ovis aries*) on St. Kilda: a consequence of parasite distribution? *Oikos* 96, 235–244.
- Illius, A.W., Gordon, I.J., Milne, J.D., Wright, W., 1995. Costs and benefits of foraging on grasses varying in canopy structure and resistance to defoliation. *Funct. Ecol.* 9, 894–903.
- Jatimlinsky, J.R., Gimenez, D.O., Bujan, A., 1997. Herbage yield tiller number and root system activity after defoliation of prairie grass (*Bromus catharticus Vahl*). *Grass Forage Sci.* 52, 52–62.
- Johnson, I.R., Thornley, J.H.M., 1984. A model of instantaneous and daily canopy photosynthesis. *Theor. Biol.* 107, 531–545.
- Keeling, M.J., 2000a. Metapopulation moments: coupling, stochasticity and persistence. *J. Anim. Ecol.* 69, 725–736.
- Keeling, M.J., 2000b. Multiplicative moments and measures of persistence in ecology. *J. Theor. Biol.* 69, 725–736.
- Keeling, M.J., Wilson, H.B., Pacala, S.W., 2000. Reinterpreting space, time lags, and functional responses in ecological models 2. *Science* 290, 1758–1761.
- Kendall, M.G., 1994. *Kendall's Advanced Theory of Statistics*. Edward Arnold, London.
- Laca, E.A., Ungar, E.D., Seligman, N., Demment, M.W., 1992. Effects of sward height and bulk density on bite dimensions of cattle grazing homogeneous swards. *Grass Forage Sci.* 47, 91–102.
- Langvatn, R., Hanley, T.A., 1993. Feeding patch choice by red deer in relation to foraging efficiency. *Oecologia* 95, 164–170.
- Marion, G., Renshaw, E., Gibson, G., 2000. Stochastic modelling of environmental variation for biological populations. *Theor. Popul. Biol.* 57, 197–217.
- Marion, G., Mao, X., Renshaw, E., Liu, J., 2002. Spatial heterogeneity and the stability of reaction states in autocatalysis. *Phys. Rev. E* 66, 051915.
- Noy-Meir, I., 1975. Stability of grazing systems: an application of predator–prey graphs. *J. Ecol.* 63, 459–481.
- Parsons, A.J., Schwinning, S., Carrere, P., 2001. Plant growth functions and possible spatial and temporal scaling errors in models of herbivory. *Grass Forage Sci.* 56, 21–34.
- Penning, P.D., Rook, A.J., Orr, R.J., 1991. Patterns of ingestive behaviour of sheep continuously stocked on monocultures of ryegrass and clover. *Appl. Anim. Behav. Sci.* 31, 237–250.
- Phillips, C.J.C., 1993. *Cattle Behaviour*. Farming Press, Ipswich.
- Rand, D.A., 1999. Correlation equations and pair approximations for spatial ecologies In: McGlade, J. (Ed.), *Advanced Ecological Theory: Principles and Applications* Blackwell Science, Oxford, UK, pp. 100–142.
- Renshaw, E., 1991. *Modelling Biological Populations in Space and Time*. Cambridge University Press, Cambridge, UK.
- Rohani, P., Keeling, M.J., Grenfell, B.T., 2002. The interplay between determinism and stochasticity in childhood diseases. *Am. Nat.* 159, 469–481.
- Schapendonk, A.H.C.M., Stol, W., Vankraalingen, D.W.G., Bouman, B.A.M., 1998. Lingra, a sink/source model to simulate grassland productivity in Europe. *Euro. J. Agron.* 9, 87–100.
- Schwinning, S., Parsons, A.J., 1999. The stability of grazing systems revisited: spatial models and the role of heterogeneity. *Funct. Ecol.* 13, 737–747.
- Ungar, E.D., 1996. Ingestive behaviour. In: Hodgson, J., Illius, A.W. (Eds.), *The Ecology and Management of Grazing Systems*. CAB International, Oxford, pp. 185–218.
- Ungar, E.D., Noymeir, I., 1988. Herbage intake in relation to availability and sward structure-grazing processes and optimal foraging. *J. Appl. Ecol.* 25, 1045–1062.
- Ungar, E.D., Ravid, N., 1999. Bite horizons and dimensions for cattle grazing herbage to high levels of depletion. *Grass Forage Sci.* 54, 357–364.
- Van Kampen, N.G., 1992. *Stochastic Processes in Physics and Chemistry*. North-Holland, Amsterdam.
- Wallisdevries, M.F., Schippers, P., 1994. Foraging in a landscape mosaic: selection for energy and minerals in free-ranging cattle. *Oecologia* 100, 107–117.
- WallisDeVries, M.F., Laca, E.A., Demment, M.W., 1998. From feeding station to patch: scaling up food intake measurements in grazing cattle. *Appl. Anim. Behav. Sci.* 60, 301–315.
- Warringa, J.W., Kreuzer, A.D.H., 1996. The effect of new tiller growth on carbohydrates, nitrogen and seed yield per ear in *Lolium perenne* L. *Ann. Bot.* 78, 749–757.
- Whittle, P., 1957. On the use of the normal approximation in the treatment of stochastic processes. *J. R. Statist. Soc. B* 19, 266–281.
- Wilmshurst, J.F., Fryxell, J.M., Farm, B.P., Sinclair, A.R.E., Henschel, C.P., 1999. Spatial distribution of serengeti wildebeest in relation to resources. *Canad. J. Zool. (Rev. Can. Zool.)* 77, 1223–1232.
- Yearsley, J., Tolcamp, B.J., Illius, A.W., 2001. Theoretical developments in the study and prediction of food intake. *Proc. Nutr. Soc.* 60, 145–156.